

We are IntechOpen, the world's leading publisher of Open Access books Built by scientists, for scientists

6,900

Open access books available

185,000

International authors and editors

200M

Downloads

Our authors are among the

154

Countries delivered to

TOP 1%

most cited scientists

12.2%

Contributors from top 500 universities



WEB OF SCIENCE™

Selection of our books indexed in the Book Citation Index
in Web of Science™ Core Collection (BKCI)

Interested in publishing with us?
Contact book.department@intechopen.com

Numbers displayed above are based on latest data collected.
For more information visit www.intechopen.com



Calorimetry Characterization of Carbonaceous Materials for Energy Applications: Review

Zulamita Zapata Benabithé

Additional information is available at the end of the chapter

<http://dx.doi.org/10.5772/intechopen.71310>

Abstract

Carbonaceous materials are of great interest for several applications in adsorption, catalysis, gases storage, and electrochemical energy storage devices because of the ability to modify their pore texture, specific surface area, and surface chemistry. Some of the most used precursors are carbon gels, biomass, carbon nanotubes, and coal. These materials can be doped or functionalized to modify their surface. Immersion calorimetry is one of the techniques used to determine the textural and chemical characterization of solids like carbonaceous materials. Immersion calorimetry provides information about the interactions that occur between solids and different immersion liquids. The measurement of heats of immersion into liquids with different molecular sizes allows for the assessment of their pore size distribution. When polar surfaces are analyzed, both the surface accessibility of the immersion liquid and the specific interactions between the solid surface and the liquid's molecules account for the total value of the heat of immersion. Zapata-Benabithé et al., Castillejos et al., Chen et al., and Centeno et al. prepared different materials and used immersion calorimetry into benzene, toluene, and/or water to correlate the external surface area of microporous solids with energy parameters such as specific capacitance or chemical surface (oxygen content, acid groups, or basic groups). This chapter will be compiling a review of the results founded about the calorimetry characterization of carbonaceous materials for energy area applications.

Keywords: immersion calorimetry, carbonaceous materials, energy applications

1. Introduction

Nowadays, the demand for electricity worldwide is supplied mainly by conventional energy sources (oil, natural gas, and coal); however, supply from renewable energy sources such as solar, wind, and others has been growing quickly since the end of the 2000's, from 18% (2000)

to 26% (2016) [1]. Although the consumption of these renewable energies has increased during the last decade, one of the main drawbacks with this type of energy is the reliability and assurance in the energy supply to the consumers, because the energy production fluctuates with the climatological conditions. For this reason, it is necessary to consider energy storage systems (ESSs) that attenuate fluctuations in power generation and can respond to variations in the demand for energy by consumers, facilitating the supply of power to the grid.

The production of electrical energy from unconventional sources coupled to an energy storage system can be more efficient because they contribute to the reduction of the environmental impact, reducing the carbon footprint and global warming and allow converting back into electrical energy when needed in different periods of time [2].

ESS can be categorized into mechanical (pumped hydroelectric storage, compressed air energy storage, and flywheels), electrochemical (conventional rechargeable batteries and flow batteries), electrical (capacitors, supercapacitors, and superconducting magnetic energy storage), thermochemical (solar fuels), chemical (hydrogen storage with fuel cells), and thermal energy storage (sensible heat storage and latent heat storage) [2]. These differ from each other on their properties, such as the type of primary energy they store, energy density and power density ranges, life cycle, application sector, and the cost of production [3].

In renewable energy-generating devices, such as wind turbines and solar panels, supercapacitors can be used for storing energy to accelerate the turbine after a period with little wind and prevent electrical dropouts in the solar panels. In the case of the transportation sector, batteries, hybrids, and hydrogen are considered as alternatives instead of fossil fuels. Supercapacitors are commonly used in cell phones and computers with backup power for the memory; besides, supercapacitors may also replace the battery in vehicles driven by internal combustion engines [4].

These devices are mainly composed by two electrodes (anode and cathode) and an electrolyte. Carbonaceous materials (carbon gels, biomass, carbon nanotubes, coal, etc.) are one of the most common materials used as electrodes due to their low cost and high superficial area ($400\text{--}2000\text{ m}^2/\text{g}$), low density ($0.3\text{--}1\text{ g/cm}^3$), and good conductivity ($5\text{--}50\text{ S/cm}$). The energy storage occurs on the surface of the electrodes, and it could be doped or functionalized to modify their superficial chemistry to improve the energy storage [5].

Nitrogen gas adsorption/desorption at 77 K, thermogravimetric analysis (TGA), differential scanning calorimetry (DSC), immersion calorimetry, X-ray diffraction (XRD), X-ray photoelectron spectra (XPS), scanning electron microscope (SEM), and Fourier-transform infrared (FT-IR) spectroscopy are the most techniques used to characterize porous materials, because they give information about textural, porous and morphology surface, and physical-chemical composition.

Immersion calorimetry is one of the techniques used to determine the textural and chemical characterization of solids like carbonaceous materials. This technique provides information about the interactions that occur between solids and different immersion liquids [6]. The measurement of heats of immersion into liquids with different molecular sizes allows for the assessment of their pore size distribution by measuring the enthalpy of immersion of the samples

into liquids of different critical dimensions. When polar surfaces are analyzed, both the surface accessibility of the immersion liquid and the specific interactions between the solid surface and the molecules of the liquid account for the total value of the heat of immersion [7].

Otherwise, DSC is a thermo-analytical technique in which the difference between the amount of heat required to increase the temperature of a sample and a reference is measured as a function of temperature [8]. DSC profiles provide information about thermal stability and thermal phase transition (transition temperature (T_g), crystalline melting temperature (T_m), and crystallization temperature (T_c) from heating curves (enthalpy; ΔH). DSC analysis can be used to understand the solid-liquid phase transition of room temperature ionic liquids (RTILs) used in energy storage devices.

In this chapter, the research results founded that the immersion calorimetry and differential scanning calorimetry as characterization techniques of carbonaceous materials for ESS such as supercapacitors will be compiling.

2. Immersion calorimetry of different liquid technique in supercapacitors application

The calorimetric technique is one of the most used techniques to perform the characterization of systems that generate or absorb thermal energy. Isothermal calorimeters exhibit a large heat exchange between the system and the environment. The system in this case is considered as a steel cell in which the liquid adsorbate and the porous material are introduced. Immersion enthalpy is a measure of the amount of heat released when a known mass of a degassed solid is completely immersed in a given liquid; the magnitude of enthalpy depends on the nature of liquid-solid interactions and the extent of available surface.

Alonso et al. [9] activated from the pitch was pyrolysis with KOH at different amount of activating agent. The activated carbons obtained were used as electrodes of supercapacitors. The activated carbons were mainly microporous, while the mesopores increased at higher amount of activating agent. The microporosity of the activated carbons was characterized by measuring the enthalpy of immersion of the samples into liquids with different size. Measurements were carried out at 20°C using dichloromethane (CH_2Cl_2 , $L = 0.33$ nm), benzene (C_6H_6 , $L = 0.41$ nm), cyclohexane (C_6H_{12}), carbon tetrachloride (CCl_4 , $L = 0.63$ nm), and tri-2,4-xylylphosphate (TXP, $L = 1.5$ nm). The increase of the amount of activating agent caused the immersion enthalpy in the liquid of the smallest size (CH_2Cl_2) to increase from 140 to 281 J/g, which is in agreement with the higher surface developed in the carbons, according to N_2 adsorption isotherm data. In the case of the sample with the lowest activating agent ratio (1/1), the immersion enthalpy in TXP were significantly lower than that obtained for the other liquids (8 J/g, respect to 109–177 J/g), indicating that the TXP molecule is not accessible to the pores developed in this sample ($d_p < 1.5$ nm). In the case of the sample with activating agent/carbon ratio of 2/1, the enthalpy of immersion in TXP was also lower than the rest of the liquids. This indicated that only a small proportion of the pores present in this sample are larger than 1.5 nm. Samples activated with a higher proportion of KOH (3/1 and 5/1) showed very

high values of immersion enthalpy into TXP, which indicated that most of the pores present in these samples are larger than 1.5 nm. The sample activated at activating agent/carbon ratio of 3/1 showed the highest specific capacitances (300–425 F/g) at different current densities (<1–90 mA/cm²) in H₂SO₄ 2 M. This behavior could be associated with the easy diffusion of the electrolyte due to a heterogeneous porous distribution, in accordance with the highest immersion enthalpies values into liquids of different sizes.

Mora et al. [10] obtained activated carbons from mesophase pitch with KOH using different proportions of the activating agent (1:1 to 5:1 KOH to carbon mass ratio) and activation temperatures (600 and 800°C) to study the effect on the textural characteristics of the resultant activated carbons and how these characteristics influenced their behavior as electrodes in supercapacitors. The textural properties of the activated carbons were studied by gas adsorption of N₂ at 77 K and CO₂ at 273 K and immersion calorimetry. Enthalpy of immersion of the samples into liquids of different critical dimensions was used to characterize the microporosity of the activated carbons. Immersion calorimetry measurements were carried out at 20°C using dichloromethane (CH₂Cl₂, L = 0.33 nm), benzene (C₆H₆, L = 0.41 nm), carbon tetrachloride (CCl₄, L = 0.63 nm), tetraisopropyl-o-titanate (TIPO, L = 1.05 nm), and tetrabutyl-o-titanate (TBOT, L = 1.3 nm). Immersion calorimetry into water was used to estimate the number of hydrophilic sites ([O + HCl]_{ΔH}) of the carbon surface according to Eq. (1) [11]:

$$[O + HCl]_{\Delta H} = [0.21 \Delta_i H_{C_6H_6} - \Delta_i H_{H_2O}] / 10 \text{ J/mmol} \quad (1)$$

The oxygen content is linked with hydrophilic character; samples with high oxygen content showed an increase of hydrophilic sites. Samples were mainly microporous (pore size ~0.9 nm). These samples showed the highest capacitances (200–400 F/g) at low current densities (0.75 mA/cm²) in 2-M H₂SO₄. However, the sample obtained at 3 of KOH:mesophase ratio and 600°C showed the highest total oxygen content (13.94 wt.%), but it did not show the highest capacity due to an increase of the equivalent series resistance (ESR). The sample activated at 5 of KOH:mesophase ratio and 700°C showed the highest capacitance at low and high current (0.75 and 75 mA/cm², respectively). This sample also showed high values of immersion enthalpies into liquids with different size, which suggests the easy access of the electrolyte into the micropores.

Centeno et al. [12] characterized 12 activated carbons with different superficial (378–1270 m²/g) and porous characteristics (micropore widths between 0.7 and 2 nm). The highest specific capacitance value obtained was 320 F/g using 2-M H₂SO₄ as electrolyte. Eq. (2) shows an empirical correlation obtained between C_o, the capacitance C (F/g) at 1 mA/cm², and the enthalpy of immersion $\Delta_i H_{C_6H_6}$ (J/g) at 293 K for 20 microporous carbons.

$$C_o = -k \Delta_i H_{C_6H_6} \quad (2)$$

The deviation of the correlation, with $k = 1.15 \pm 0.1$ (F/J), could be related with specific chemical reactions of the acid with surface groups and to the relatively strong physical interaction between water and the surface oxygen atoms. The enthalpy of immersion of benzene also depends on the

structural parameters such as microporous (S_{mi}) and external (S_e) surface areas and volume (W). Eq. (2) can be used to evaluate empirically the performance of a given carbon as a capacitor.

Sevilla et al. [13] prepared templated mesoporous carbons (TMCs) to be used as supercapacitors. The double layer capacity formed on their surface corresponds to 0.14 F/m² in aqueous electrolytes, such as H₂SO₄ and KOH, and 0.06 F/m² for the aprotic medium (C₂H₅)₄NBF₄/CH₃CN. The effective surface area was determined by independent techniques from Eq. (3): analysis of the nitrogen isotherms by the comparison plot (S_{comp}) and DFT (S_{DFT}) and based on the enthalpy of immersion into dilute aqueous solution of phenol (S_{phenol}) and benzene ($S_{benzene}$).

$$S_{av} = (S_{comp} + S_{phenol} + S_{benzene} + S_{DR})/4 \quad (3)$$

The total surface area can be as high as 1500–1600 m²/g. The relatively low amount of surface oxygen in the present TMCs, as opposed to activated carbons, reduces the contribution of pseudo-capacitance effects and limits the gravimetric capacitance to 200–220 F/g for aqueous electrolytes. In the case of nonaqueous electrolyte, it rarely exceeds 100 F/g. The ionic mobility did not improved due to the mesoporous presence of these TMCs compared with activated carbons of pore widths above 1.0–1.3 nm.

Fernández et al. [14] obtained mesoporous materials from mixtures of poly(vinyl alcohol) with magnesium citrate carbonized and evaluated their performance as electrodes in supercapacitors. The highest specific capacitance (C_o) at low current density (1 mA/cm²) values was 180 F/g in 2 M H₂SO₄ electrolyte and around 100 F/g in 1 M (C₂H₅)₄NBF₄ in acetonitrile. The specific surface area (S_{av}) was calculated as an average of the several specific surface area values; they were estimated by employing different procedures such as comparison plot (S_{comp}) and based on the enthalpy of immersion into phenol (S_{phenol}) and benzene ($S_{benzene}$), according to Eq. (4).

$$S_{av} = (S_{comp} + S_{phenol} + S_{benzene})/3 \quad (4)$$

The addition up to approximately 40% of MgO to the raw mixture gradually increased the average specific surface area of the resulting carbons up to approximately 1300 m²/g. C_o of different mesoporous carbons obtained in aqueous 2-M H₂SO₄ solution and aprotic electrolyte 1-M (C₂H₅)₄NBF₄/CH₃CN were correlated with S_{av} . The relationship of C_o vs. S_{av} showed a linear increase of the limit specified both in an acid medium and aprotic. The lines through the origin correspond to 0.14 F/m² in aqueous solution and of 0.07 F/m² in the aprotic electrolyte.

Ruiz et al. [15] prepared carbonaceous materials from naphthalene-derived mesophase pitch. These were chemically activated using (3:1) KOH to carbon mass ratio at 700°C for 1 h under nitrogen flow. The activated carbon was thermally treated at 600 and 1000°C under nitrogen flow. The microporosity of the electrodes was characterized by measuring the enthalpy of immersion of the samples into liquids of different critical dimensions. Measurements were carried out at 20°C using dichloromethane (0.33 nm) and tri-2,4-xylylphosphate, TXP (1.5 nm). In the thermal treatment at 600°C, a slight reduction in the capacity to adsorb the nitrogen was showed. The total pore volume was reduced from 0.85 to 0.80 cm³/g, and microporous surface

area was reduced, S_{mic} from 1531 to 1407 m²/g (8% reduction compared to original activated carbon). The thermal treatment at 1000°C generated a decrease of the total pore volume up to 0.66 cm³/g, and the S_{mic} decreased up to 1318 m²/g (14%). The average pore size reduced considerably. After thermal treatment, the heat of immersion obtained for CH₂Cl₂ and TXP diminished respect to the original activated carbon for both temperatures, at 600°C from 197 to 206 J/g with CH₂Cl₂ and at 1000°C from 82 to 43 J/g with TXP. These could be related with the presence of constrictions and secondly due to the reduction in the average pore size. The specific capacitance of the original activated carbon was 309 F/g in 1 M H₂SO₄, while the specific capacitance for the activated carbons treated thermally diminished up to 85 F/g for 600°C and 196 F/g for 1000°C. The reason could be the formation of physical constrictions at the entrance of the porous network which makes it more difficult for the electrolyte to gain access.

Olivares-Marín et al. [16] produced activated carbon with KOH from cherry stones wastes for electrode material in supercapacitors. The chemical activation of cherry stones was carried out by different agents such as H₃PO₄, ZnCl₂, and KOH. The activated carbons prepared with KOH showed the highest total specific surface area TSA ($S_{mi} + S_e$) (1100–1300 m²/g) and also the conductivities 1 and 2 S/cm. The materials obtained by carbonization of a mixture of KOH and cherry stones with a ratio 3:1 at 800 and 900°C (carbons K3–800 and K3–900) consists mainly of micropores (width < 2 nm). Their surface areas are respectively 1244 m²/g and 1039 m²/g. The carbonaceous material obtained with KOH/cherry stones ratio of 1:1 and 3:1 at 800°C (K1–800 and K3–800) showed similar porosity. However, immersion calorimetry with different molecular probes indicated significant differences in the micropore size distribution. The comparison of the immersion enthalpies into water $\Delta_i H(H_2O)$ and into benzene $\Delta_i H(C_6H_6)$ suggested that the surface oxygen density for cherry stones-based materials varied between 1.2 and 3.0 $\mu\text{mol}/\text{m}^2$. The specific enthalpy of immersion into water, $h_{i[H_2O]}$ Eq. (5), was around –0.04 to –0.06 J/m².

$$h_{i[H_2O]} = \frac{\Delta_i H_{[H_2O]}}{TSA} [=] \frac{J/g}{m^2/g} [=] \frac{J}{m^2} \quad (5)$$

The specific capacitances values (C) at low current density as high as 230 F/g in aqueous electrolyte 2-M H₂SO₄ and 120 F/g in the aprotic medium 1-M (C₂H₅)₄NBF₄/acetonitrile. The correlation between C and TSA showed a specific surface-related capacitance [C (F/g)/TSA (m²/g)] around 0.17 F/m² in H₂SO₄ electrolyte and 0.09 F/m² in (C₂H₅)₄NBF₄/acetonitrile medium. The highest value in the acidic electrolyte showed an extra contribution from certain functional surface complexes (containing mainly oxygen and nitrogen) in the form of quick oxidation/reduction reactions that promoted the pseudo-capacitance effects to be added to the purely double layer capacitance associated with the surface area. In the case of the aprotic electrolyte, the contribution did practically not depend on the chemistry of the carbon surface.

Garcia-Gomez et al. [17] prepared cylindrical carbon monoliths, and they studied their behavior as electrodes for supercapacitors. The porosity of the carbon monoliths was characterized by N₂ adsorption at 77 K and by immersion calorimetry at 293 K. The total surface area was calculated from the average values of comparison method (S_{comp}), immersion calorimetry into aqueous solution of phenol (S_{phenol}), and the Dubinin-Radushkevich approach (S_{DR}), from Eq. (6) instead of surface area estimated from the BET equation (S_{BET}).

$$S_{av} = (S_{comp} + S_{phenol} + S_{DR})/3 \quad (6)$$

S_{BET} underestimates the total surface area for carbons with average micropore size below 0.8–0.9 nm. The interfacial capacitance was 14 $\mu\text{F}/\text{cm}^2$, obtained in KOH electrolyte, for a specific capacitance of 150 F/g at low current densities (1 mA/cm² or 10 mA/g) and the specific surface area, $S_{total} = 1086 \text{ m}^2/\text{g}$. According to Ref. [18], the double layer capacitance per unit of micropore surface area was found to be very close to that of carbon basal plane (about 15–20 $\mu\text{F}/\text{cm}^2$). Moreover, the chemical nature of carbon surface could be estimated from the specific enthalpy of immersion into water $-\Delta_i H_{H_2O}$ (J/g). The low value of the $-\Delta_i H_{H_2O}/S_{total}$ ratio ($-0.023 \text{ J}/\text{m}^2$) suggests that the monolith surface has nonoxygenated functionalities.

Sánchez-González et al. [19] selected a commercial activated carbon (Norit® C-Granular) and treated it under N₂ at 700, 800, and 900°C during 2 h. The activated carbons were evaluated electrochemically as electrodes of supercapacitors in aqueous (2 M H₂SO₄) and organic (1 M (C₂H₅)₄NBF₄/CH₃CN) electrolytes. The microporosity characterization was based on Dubinin's theory, micropore volume (W_0), the average width (L_0) of the locally slit-shaped micropores and the surface area of the micropore walls (S_{mi}), the total pore volume (V_p), and the external surface (S_e) from N₂ adsorption at 77 K isotherm. Other methods such as the comparison plot (S_{comp}) and the density functional theory (S_{DFT}) were used. The average surface area was calculated from Eq. (7).

$$S_{av} = (S_{totDR} + S_{comp} + S_{DFT})/3 \quad (7)$$

The density of surface oxygenated functionalities was estimated by the enthalpies of immersion into water and into benzene at 293 K. After heat treatment did not change significantly the pore structure of carbons, the surface oxygen density, presence of carboxylic acid groups, diminished (9.6 to 4.5–5.6 $\mu\text{mol}/\text{m}^2$). The commercial activated carbon showed relatively high surface area (727 m^2/g) but a poor electrochemical performance in both aqueous and aprotic media. The cyclic voltammograms based on carbons C700–C900 showed a regular box-like behavior of an ideal capacitor. The rectangular shape was well preserved over a wide range of scan rates (1–50 mV/s), which indicates a quick charge propagation. High gravimetric capacitances were obtained from galvanostatic charge–discharge cycling at 1 mA/cm² from 124 to 173 F/g in the aqueous H₂SO₄ electrolyte and around 74–80 F/g in the aprotic medium.

Figure 1 shows a relationship between the surface-related capacitances (C_o/S_{av}) with electric conductivity (S/m). The sample C900 showed the lowest C_o/S_{av} with the highest electric conductivity, and this behavior could be related to the enhancement in the structural order by thermal annealing of the pseudographitic carbonaceous layers. In aqueous and aprotic electrolytes, the sample C900 showed a limited effect on the capacitor capacity for energy storage, but results in power density was almost four times higher than C700.

Zapata-Benabithé et al. [20] obtained carbon aerogels by carbonizing organic aerogels prepared by polycondensation reaction of resorcinol or pyrocatechol with formaldehyde. They are KOH activated at two KOH/carbon ratios to increase pore volume and surface area, and selected samples were surface treated to introduce oxygen and nitrogen functionalities.

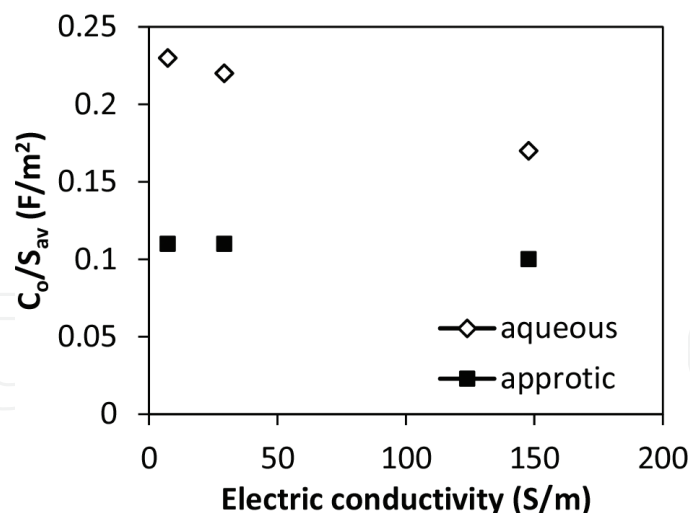


Figure 1. Relationship between the surface-related capacitances and electric conductivity.

The samples were evaluated as electrodes for supercapacitors in 1-M H_2SO_4 . The samples were characterized by N_2 and CO_2 adsorption at -196 and 0°C , respectively, immersion calorimetry, temperature-programmed desorption, and X-ray photoelectron spectroscopy in order to determine their surface area, porosity, and surface chemistry. Two series of samples were obtained: one micro-mesoporous and another basically microporous. After KOH activation, the specific surface area (from BET equation) showed values up to $1935 \text{ m}^2/\text{g}$. Immersion enthalpies into benzene, $-\Delta H_{\text{benz}}$, water, and $-\Delta H_{\text{water}}$, were used to determine the hydrophobicity (HF) of the samples according to Eq. (8).

$$HF = 1 - (\Delta H_{\text{water}} / \Delta H_{\text{benz}}) \quad (8)$$

The hydrophobicity factor varied between -0.12 and 0.75 for the activated and functionalized carbon aerogels. The relationship between the hydrophobicity and the surface (O_{xps}) and total (O_{TPD}) oxygen content of the samples diminished linearly with an increase in the oxygen content. The increase of the oxygen content improved the wettability of the carbon surface by the electrolyte, facilitating the EDL formation. However, this advantage can be offset by the binding of oxygen polar groups (mainly carboxyl groups) with water molecules, hindering and retarding the migration of the electrolyte into the pores and thereby increasing the ohmic resistance. One of the samples with the highest gravimetric capacitance in 1-M H_2SO_4 , 221 F/g at 0.125 A/g , was obtained with micro-mesoporous characteristics and the highest oxygen functionalities.

Elmouwahidi et al. [21] prepared activated carbons by KOH activation of argan seed shells (ASS), and the activated carbon with the largest surface area was superficially treated to introduce oxygen and nitrogen functionalities. Samples were characterized by N_2 and CO_2 adsorption at -196 and 0°C and immersion calorimetry into benzene and water. Immersion enthalpies into benzene, ΔH_{benz} , were used to determine the surface area of the activated carbons, S_{benz} . Benzene molecule has no specific interactions with surface groups, considering the immersion enthalpy into benzene of a nonporous graphitized carbon black to be 0.114 J/m^2 [22]. The hydrophobicity of samples was determined from Eq. (8). The Dubinin-Radushkevich (DR)

equation was applied to the N_2 and CO_2 isotherms to obtain the micropore volume, $W_0(N_2)$ and $W_0(CO_2)$, respectively. All samples showed $W_0(N_2) > W_0(CO_2)$, indicating an absence of constrictions at micropore entrances and hence complete accessibility to N_2 molecules at $-196^\circ C$. The apparent surface area (S_{BET}) and S_{benz} values were similar, due to the dimensions of N_2 (0.36 nm) and benzene (0.37 nm) are almost identical, and the micropore width allowed the accommodation of one N_2 monolayer on each micropore wall. The hydrophobicity varied between -0.21 and 0.53 and decreased as a consequence of the fixation of oxygen functionalities with large polarity like carboxyl groups. Activated carbon aerogel superficially treated with oxygen functional groups showed the lowest specific capacitance at 0.125 and 1 A/g and 259 and 135 F/g, respectively, in $1\text{-M } H_2SO_4$. This behavior could be expressed by the presence of surface carboxyl groups hindering electrolyte diffusion into the highly polar pores.

Zapata-Benabith et al. [23] studied the effect of the Boron dopant (boric and phenyl boronic acids) and drying method (supercritical, freeze, microwave oven, and vacuum drying) on the surface physics and chemistry of B-doped resorcinol-formaldehyde gels and their electrochemical behavior. The surface characteristics were studied by N_2 and CO_2 adsorption at -196 and $0^\circ C$, respectively, and immersion calorimetry into benzene and water. The N_2 adsorption-desorption isotherms at $-196^\circ C$ were type IV and showed a type H2 hysteresis cycle for all B-doped carbon gels obtained. The micropore volume ($W_0(N_2)$) and specific surface area (S_{BET}) values were similar for all samples (~ 0.23 cm³/g and 560 – 590 m²/g, respectively), except the samples with phenyl boronic acids dried in freeze and vacuum drying oven. This behavior suggests that the drying method has practically no influence on porous characteristics. The surface area from enthalpy of immersion into benzene was determined (S_{imm}) from Eq. (9) and compared with S_{BET} values.

$$S_{C_6H_6} = \frac{\Delta H_{iC_6H_6}}{\Delta h_{C_6H_6}} \quad (9)$$

The results showed that the $S_{imm} > S_{BET}$ in all samples. The S_{BET} can underestimate with respect to the S_{imm} , because of the restricted diffusion of N_2 at $-196^\circ C$ in very narrow micropores or in those with constrictions at their entrance, whereas benzene molecules can access all micropores because of the much higher temperature ($30^\circ C$) at which immersion took place.

The gravimetric capacitances (C_{CP}) from chronopotentiometry technique were obtained in aqueous media $1\text{-M } H_2SO_4$. The interfacial or areal capacitance, IC_{CP} , was calculated from C_{CP} and S_{imm} values. The selection of S_{imm} was due to it gave a more realistic value of the surface area of the B-doped carbon gels. Most of these values are in fairly good agreement with the interfacial capacitance of a clean graphite surface, 20 $\mu F/cm^2$, and with the value range between 20 and 30 $\mu F/cm^2$ reported for different carbons, indicating a good accessibility to the microporosity of the carbon gels.

The relationship between IC_{CP} and S_{imm} for B-doped carbon gels showed a good linear agreement (correlation coefficient of 0.927). The decrease in IC_{CP} with a larger surface area could be explained by the lower EDL capacitance on graphite basal planes versus edges [24]. A rise in the S_{imm} increases the proportion of surface sites on basal planes on the walls

of the slit-shaped micropores versus edge sites mainly on the external surface, reducing the interfacial capacitance. IC_{CP} tends to increase with a higher areal oxygen concentration (O_{XPS}), because of the increase in pseudocapacitance effects produced by the surface oxygen functionalities, enhancing the total capacitance.

3. Differential scanning calorimetry technique in supercapacitors application

Electrochemical energy storage devices operate at room temperature and environment conditions; therefore, differential scanning calorimetry has used to characterize the thermal decomposition behavior of solid polymer electrolytes and electrodes (metal oxides, polymer and carbon) used in supercapacitors applications.

Ghaemi et al. [25] prepared MnO_2 materials (γ and layered types) by a novel ultrasonic aided procedure and studied the charge storage mechanism of the prepared samples as a function of the physisorbed water. The water content of manganese dioxide is considered as one of the key factors in the electrochemical performance of MnO_2 . The hydrous regions in the electrode provide the kinetically facile sites needed for the charge-transfer reaction and cation diffusion. To prepare hydrous manganese oxide with different amount of water contents, the samples were thermal treated at 70, 100, and 150°C for 2 h in air. Thermal gravimetric analysis (TGA) and differential scanning calorimetry (DSC) were employed to characterize the water content of the samples. TGA and DSC plots were carried out in air atmosphere with a heating rate of 10°C/min. The DSC analysis showed a wide and steep endothermic peak around 100°C for $\gamma 25$. The peak was stronger for L25 than $\gamma 25$ and also shifts toward higher temperature (~125°C) which indicated that the physically adsorbed water is strongly bonded to the porous surface of L25. The heat-treatment temperature decreases the physisorbed water. The cyclic voltammograms (CV) in aqueous 0.5-M Na_2SO_4 electrolyte within a potential window of 0.0 to +1.0 V versus Ag/AgCl, for both samples, showed almost rectangular and symmetric shape characteristics of a supercapacitor. The specific capacitances values from CV, at a scan rate of 5 mV/s in 0.5 M Na_2SO_4 at pH 3.3 and 6, were ranged between 100 and 350 F/g. The specific capacitances values decayed gradually through both increasing solution pH and heat-treatment temperatures. The pseudocapacitance diminished due to a reduction of the amount of physisorbed water, which is associated with a decline of electrochemical active sites within the electrode. The L25 series showed higher specific capacitances values in comparison with $\gamma 25$, which could be related to the higher amount of the physisorbed water.

Zeng et al. [26] prepared a sheet of Vanadium oxides (V_6O_{13}) from NH_4VO_3 powders to further use it as electrodes of supercapacitors. Vanadium oxides have been widely used as cathode materials for lithium ion battery because of their high-specific capacitance and good cyclability. V_6O_{13} has a blended valence of V(IV) and V(V) which is favorable for increasing the electronic conductivity of the material and a promising material in supercapacitors because of its lower cost compared to RuO_2 . Thermogravimetric and differential scanning calorimeter (TGA–DSC) were used to study the thermal behavior of NH_4VO_3 powders. From TGA

curve, there were two weight losses in the ranges of 185–235°C and 290–320°C, which corresponding to endothermic peaks showed on the DSC curve. An extra endothermic peak centered at 670°C was observed on DSC curve. The melt temperature for V_6O_{13} was considered at 800°C. Electrochemical properties of the prepared samples were determined by cyclic voltammetry (CV) and charge–discharge tests in aqueous electrolyte (1 M $NaNO_3$, KNO_3 , Na_2SO_4 , and $LiNO_3$). The CV curves showed a relatively like rectangular and symmetrical shape thus indicating ideal capacitive property for V_6O_{13} . The $NaNO_3$ electrolyte exhibited better specific capacitance, 285 F/g (50 mA/g) and 215 F/g (200 mA/g).

Fan et al. [27] developed a novel hierarchical porous carbon membranes using as the source of carbon polyacrylonitrile (PAN), polyvinylpyrrolidone (PVP) as an additive, and N,N-dimethylformamide (DMF) as a solvent. The membranes were prepared with the casting solutions by spin coating coupled with a liquid–liquid phase separation technique at room temperature. The morphology and nanostructure of the membranes were tuned by adjusting the additive concentrations in the casting solutions (0–5 wt.%). Later, the membranes were pre-oxidized, carbonized, and finally modified with nitric acid. Thermogravimetric analysis (TGA) and differential scanning calorimetry (DSC) of the samples were performed in a nitrogen atmosphere with a heating rate of 10°C/min in the temperature range of 25–900°C. The DSC data showed that there were two broad exothermic peaks in ~270 and ~700°C. The significant weight loss stage below ~270°C is mainly due to the loss of crystal water and partial dehydrogenation and cross-linking. The weight loss in the temperature range of 270–470°C can be attributed to the decomposition of PVP in the membrane. At temperature exceeding ~470°C, the weight loss can be assigned to the carbonization of PAN accompanying with further dehydrogenation and partial denitrogenation. The sample prepared with 0.3 wt.% of PVP showed the most reasonable hierarchical pore structure (2–5, 5–50, and >100 nm), high BET surface area (332.9 m²/g), big total pore volume (0.233 m³/g), and the best electrochemical performance in 2-M KOH aqueous solution. The specific capacitance was 278 and 206 F/g at 5 and 50 mA/cm², respectively, indicating the suitability of the material as electrode materials for supercapacitors.

The desirable properties of polymer electrolytes are high ionic conductivity, good temperature, and environmental stability, as well as thin film processability. However, its conductivity is lower than liquid electrolytes and high sensitivity to water are limitation to become viable materials for electrochemical energy conversion and storage devices [28].

Gao and Lian [28] characterized the structural and thermal behavior of solid polymer electrolyte using poly(vinyl alcohol) (PVA) and studied the factors contributing to the proton conductivity. Two solid polymer electrolytes were prepared mixing a 15 wt.% PVA solution with a heteropoly acid solution at 32.5 wt.%, one with $H_4SiW_{12}O_{40} \cdot xH_2O$ (PVA-SWA) and the other one with $H_3PW_{12}O_{40} \cdot xH_2O$ (PVA-PWA) and 66 wt.% de-ionized water. The PVA-PWA and PVA-SiWA precursors were combined in equal volumes for a mixed polymer electrolyte (PVA-Mix). Differential scanning calorimetry (DSC) analyses were performed with a scan rate of 10°C/min in nitrogen purged cell over a temperature range from 10 to 150°C. The DSC thermograms for PVA-Mix as well as for its individual components (PVA, PWA, and SiWA) showed that the glass transition temperature (T_g) of pure PVA was found around

84°C. At higher temperatures, there was one endothermic peak for PWA but a split peak for SiWA. In the case of PVA-Mix, two clear endothermic peaks were observed. The water content decreased in the early phase of the temperature scan for all samples. The endothermic peaks could be interpreted as a phase transition or as the escape of certain form of water. The crystallized water in the PVA matrix is more stable than PWA or SiWA, due to the complete release of crystallized protonated water required a higher temperature (122°C for PVA-Mix, respect to 78°C for PVA and 106°C for SiWA). The solid polymer PVA-Mix has been used as an electrolyte with RuO₂/TiO₂ electrodes [29], due to its very good proton conductivity (0.013 S/cm) and stability at environment temperature and relative humidity, forming a solid cell with a thickness of 0.2 mm. At a voltage scan rate of 500 mV/s, the CV profiles were still quite rectangular and showed a capacitance of 50 mF/cm² in the cell, which suggests that the electrolyte is viable for high rate capacitive devices. The polymer electrolyte not only acted as proton conductor but also facilitated the oxidation and reduction reactions of the electrodes.

Liew et al. [30] investigated the effect of ionic liquid on the PVA-CH₃COONH₄ polymer electrolytes in supercapacitor application. Ionic liquid-based poly(vinyl alcohol) polymer electrolytes were prepared by means of solution casting. PVA was initially dissolved in distilled water. The weight ratio of PVA:CH₃COONH₄ was kept at 70:30, and different weight ratio of BmImCl (0–60 wt.%) was thus added into the PVA-CH₃COONH₄ mixture to prepare ionic liquid-based polymer electrolyte. The increment of BmImCl enhances the ionic conductivity, due to strong plasticizing effect of ionic liquid. The glass transition temperature (T_g) of the electrolytes was determined from DSC analysis. This study indicated the phase transition of a polymer matrix in the amorphous region, from a hard glassy phase into a flexible and soft rubbery characteristic. The T_g decreased further with addition of ionic liquid. This behavior denoted that the plasticizing effect of CH₃COONH₄ dominates the temporary interactive coordination. This plasticizing effect softens the polymer backbone and thus produces flexible polymer backbone. Polymer electrolyte containing 50 wt.% of BmImCl offered the maximum ionic conductivity of (7.31 ± 0.01) mS/cm at 120°C. The EDLC containing the most conducting polymer electrolyte was assembled and could be charged up to 4.8 V. The specific capacitance of 28.36 F/g was achieved with better electrochemical characteristic in cyclic voltammogram. The higher ion concentration favors the ion migration within the polymer electrolyte (known as separator in EDLC) and promotes the charge accumulation at the electrolyte-electrode boundary. The inclusion of ionic liquid not only improved the interfacial contact between electrode and electrolyte but also increases the electrochemical property of supercapacitors.

Yang et al. [31] obtained a promising ionic liquid-gelled polymer electrolyte (GPE) based on semi-crystal polyvinylidene fluoride (PVDF), amorphous polyvinyl acetate (PVAc), and ionic conductive 1-butyl-3-methylimidazolium tetrafluoroborate (BMIMBF₄) via solution-casting method. The thermal stability of the GPEs was measured by thermogravimetric/differential scanning calorimetry (TG/DSC). The PVDF/PVAc/IL (IL, 50 wt.%) GPE film presents good thermal stability (~300°C), wide electrochemical window (>4.0 V), and acceptable ionic conductivity (2.42 × 10⁻³ S/cm at room temperature) as well. The electrodes were prepared from commercial-activated carbon blended with acetylene black and PTFE at the mass

ratio of 85:10:5 wt.%. The solid-state capacitor was assembled with one piece of electrolyte film was placed on one activated carbon electrode surface, and the other symmetrical electrode was placed over the gel film to form a “Sandwich Structure”, subsequently sealed into a commercial CR1016 coin cell mold. A 3.0-V C/C solid-state capacitor cell using this GPE film showed a specific capacitance of 93.3 F/g at the current density of 200 mA/g and could retain more than 90% of the initial capacitance after 5000 charge–discharge cycles.

Peng et al. [32] prepared gel electrolytes from zwitterionic nature of poly (propylsulfonate dimethylammonium propylmethacrylamide) (PPDP) for solid-state supercapacitors. An ideal gel electrolyte should allow a high ion migration rate, reasonable mechanical strength, and robust water retention ability at the solid state for ensuring excellent work durability. The differential scanning calorimetry (DSC) showed PPDP has high water retention ability. No endothermic peak could be observed in the thermogram during the heating of PPDP without water and samples with mole ratio of H₂O to PDP of 6:1 and 7:1 from –35 to 60°C, suggesting that the polyzwitterion itself does not contribute to the thermal transition behavior. However, an endothermic peak is observed as the mole ratio of H₂O to PDP increases to 8:1, which means that the freezable water can be detected in the system when all binding sites of the polyzwitterion are saturated by water molecules. The zwitterionic gel electrolyte were assembled with graphene-based solid-state supercapacitor and reached a volume capacitance of 300.8 F/cm³ at 0.8 A/cm³ with a rate capacity of only 14.9% capacitance loss as the current density increases from 0.8 to 20 A/cm³.

Author details

Zulamita Zapata Benabithé

Address all correspondence to: zulamita.zapata@upb.edu.co

Grupo de Energía y Termodinámica, Facultad de Ingeniería Química, Escuela de Ingeniería, Universidad Pontificia Bolivariana, Antioquia, Colombia

References

- [1] Enerdata, Global Energy Statistical Yearbook 2017, France, 2011. <https://yearbook.enerdata.net/renewables/renewable-in-electricity-production-share.html>
- [2] Luo X, Wang J, Dooner M, Clarke J. Overview of current development in electrical energy storage technologies and the application potential in power system operation. *Applied Energy*. 2015;**137**:511-536. DOI: 10.1016/j.apenergy.2014.09.081
- [3] Kötz R, Hahn M, Gallay R. Temperature behavior and impedance fundamentals of supercapacitors. *Journal of Power Sources*. 2006;**154**:550-555. DOI: 10.1016/j.jpowsour.2005.10.048
- [4] Hauge HH, Presser V, Burheim O. In-situ and ex-situ measurements of thermal conductivity of supercapacitors. *Energy*. 2014;**78**:373-383. DOI: 10.1016/j.energy.2014.10.022

- [5] Lota G, Centeno T, Frackowiak E, Stoeckli F. Improvement of the structural and chemical properties of a commercial activated carbon for its application in electrochemical capacitors. *Electrochimica Acta*. 2008;**53**:2210-2216. DOI: 10.1016/j.electacta.2007.09.028
- [6] Vargas DP, Giraldo L, Moreno-Piraján JC. Calorimetric study of functionalized carbonaceous materials. *Thermochimica Acta*. 2015;**611**:20-25
- [7] Silvestre-Albero J, Gómez de Salazar C, Sepúlveda-Escribano A, Rodríguez-Reinoso F. Characterization of microporous solids by immersion calorimetry. *Colloids and Surfaces A: Physicochemical and Engineering Aspects*. 2001;**187-188**:151-165. DOI: 10.1016/S0927-7757(01)00620-3
- [8] Höhne G, Hemminger W, Flammersheim H-J. *Differential Scanning Calorimetry*. 2nd ed. Berlin: Springer; 2003
- [9] Alonso A, Ruiz V, Blanco C, Santamaría R, Granda M, Menéndez R, et al. Activated carbon produced from Sasol-Lurgi gasifier pitch and its application as electrodes in supercapacitors. *Carbon New York*. 2006;**44**:441-446. DOI: 10.1016/j.carbon.2005.09.008
- [10] Mora E, Ruiz V, Santamaría R, Blanco C, Granda M, Menéndez R, et al. Influence of mesophase activation conditions on the specific capacitance of the resulting carbons. *Journal of Power Sources*. 2006;**156**:719-724. DOI: 10.1016/j.jpowsour.2005.06.025
- [11] Stoeckli F. Water adsorption in activated carbons of various degrees of oxidation described by the Dubinin equation. *Carbon New York*. 2002;**40**:969-971. DOI: 10.1016/S0008-6223(02)00087-8
- [12] Centeno TAT, Stoeckli F. On the specific double-layer capacitance of activated carbons, in relation to their structural and chemical properties. *Journal of Power Sources*. 2006;**154**:314-320. DOI: 10.1016/j.jpowsour.2005.04.007
- [13] Sevilla M, Álvarez S, Centeno TA, Fuertes AB, Stoeckli F. Performance of templated mesoporous carbons in supercapacitors. *Electrochimica Acta*. 2007;**52**:3207-3215. DOI: 10.1016/j.electacta.2006.09.063
- [14] Fernández JA, Morishita T, Toyoda M, Inagaki M, Stoeckli F, Centeno TA. Performance of mesoporous carbons derived from poly(vinyl alcohol) in electrochemical capacitors. *Journal of Power Sources*. 2008;**175**:675-679. DOI: 10.1016/j.jpowsour.2007.09.042
- [15] Ruiz V, Blanco C, Granda M, Menéndez R, Santamaría R. Effect of the thermal treatment of carbon-based electrodes on the electrochemical performance of supercapacitors. *Journal of Electroanalytical Chemistry*. 2008;**618**:17-23. DOI: 10.1016/j.jelechem.2008.02.016
- [16] Olivares-Marín M, Fernández JA, Lázaro MJ, Fernández-González C, Macías-García A, Gómez-Serrano V, et al. Cherry stones as precursor of activated carbons for supercapacitors. *Materials Chemistry and Physics*. 2009;**114**:323-327. DOI: 10.1016/j.matchemphys.2008.09.010
- [17] Garcia-Gomez A, Miles P, Centeno TA, Rojo JM. Uniaxially oriented carbon monoliths as supercapacitorelectrodes. *Electrochimica Acta*. 2010;**55**:8539-8544. DOI: 10.1016/j.electacta.2010.07.072

- [18] Shi H. Activated carbons and double layer capacitance. *Electrochimica Acta*. 1996;**41**: 1633-1639. DOI: 10.1016/0013-4686(95)00416-5
- [19] Sánchez-González J, Stoeckli F, Centeno TA. The role of the electric conductivity of carbons in the electrochemical capacitor performance. *Journal of Electroanalytical Chemistry*. 2011;**657**:176-180. DOI: 10.1016/j.jelechem.2011.03.025
- [20] Zapata-Benabith Z, Carrasco-Marín F, Moreno-Castilla C. Preparation, surface characteristics, and electrochemical double-layer capacitance of KOH-activated carbon aerogels and their O- and N-doped derivatives. *Journal of Power Sources*. 2012;**219**:80-88. DOI: 10.1016/j.jpowsour.2012.07.0
- [21] Elmouwahidi A, Zapata-Benabith Z, Carrasco-Marín F, Moreno-Castilla C. Activated carbons from KOH-activation of argan (*Argania spinosa*) seed shells as supercapacitor electrodes. *Bioresource Technology*. 2012;**111**:185-190. DOI: 10.1016/j.biortech.2012.02.010
- [22] Denoyel R, Fernandez-Colinas J, Grillet Y, Rouquerol J. Assessment of the surface area and microporosity of activated charcoals from immersion calorimetry and nitrogen adsorption data. *Langmuir*. 1993;**9**:515-518. DOI: 10.1021/la00026a025
- [23] Zapata-Benabith Z, Moreno-Castilla C, Carrasco-Marín F. Influence of the boron precursor and drying method on surface properties and electrochemical behavior of boron-doped carbon gels. *Langmuir*. 2014;**30**:1716-1722. DOI: 10.1021/la404667y
- [24] Kinoshita K. *Carbon, Electrochemical and Physicochemical Properties*. Canada: John Wiley & Sons, Inc; 1988
- [25] Ghaemi M, Ataherian F, Zolfaghari A, Jafari SM. Charge storage mechanism of sonochemically prepared MnO₂ as supercapacitor electrode: Effects of physisorbed water and proton conduction. *Electrochimica Acta*. 2008;**53**:4607-4614. DOI: 10.1016/j.electacta.2007.12.040
- [26] Zeng HM, Zhao Y, Hao YJ, Lai QY, Huang JH, Ji XY. Preparation and capacitive properties of sheet V₆O₁₃ for electrochemical supercapacitor. *Journal of Alloys and Compounds*. 2009;**477**:800-804. DOI: 10.1016/j.jallcom.2008.10.100
- [27] Fan H, Ran F, Zhang X, Song H, Jing W, Shen K, et al. A hierarchical porous carbon membrane from polyacrylonitrile/polyvinylpyrrolidone blending membranes: Preparation, characterization and electrochemical capacitive performance. *Journal of Energy Chemistry*. 2014;**23**:684-693. DOI: 10.1016/S2095-4956(14)60200-X
- [28] Gao H, Lian K. Characterizations of proton conducting polymer electrolytes for electrochemical capacitors. *Electrochimica Acta*. 2010;**56**:122-127. DOI: 10.1016/j.electacta.2010.09.036
- [29] Gao H, Tian Q, Lian K. Polyvinyl alcohol-heteropoly acid polymer electrolytes and their applications in electrochemical capacitors. *Solid State Ionics*. 2010;**181**:874-876. DOI: 10.1016/j.ssi.2010.05.006
- [30] Liew CW, Ramesh S, Arof AK. Good prospect of ionic liquid based-poly(vinyl alcohol) polymer electrolytes for supercapacitors with excellent electrical, electrochemical and thermal properties. *International Journal of Hydrogen Energy*. 2014;**39**:2953-2963. DOI: 10.1016/j.ijhydene.2013.06.061

- [31] Yang L, Hu J, Lei G, Liu H. Ionic liquid-gelled polyvinylidene fluoride/polyvinyl acetate polymer electrolyte for solid supercapacitor. *Chemical Engineering Journal*. 2014;**258**:320-326. DOI: 10.1016/j.cej.2014.05.149
- [32] Peng X, Liu H, Yin Q, Wu J, Chen P, Zhang G, et al. A zwitterionic gel electrolyte for efficient solid-state supercapacitors. *Nature Communications*. 2016;**7**:11782. DOI: 10.1038/ncomms11782

IntechOpen

IntechOpen